12th International Symposium on Turbulence and Shear Flow Phenomena (TSFP12)
Osaka, Japan, July 19–22, 2022

NUMERICAL ANALYSIS OF THE FLOW DYNAMICS BEHIND NON-CIRCULAR BLUFF-BODIES

Agnieszka Wawrzak
Department of Thermal Machinery
Czestochowa University of Technology
Al. Armii Krajowej 21, 42-201 Czestochowa, Poland
agnieszka.wawrzak@pcz.pl

Robert Kantoch
Department of Thermal Machinery
Czestochowa University of Technology
Al. Armii Krajowej 21, 42-201 Czestochowa, Poland
robert.kantoch@pcz.pl

Artur Tyliszczak
Department of Thermal Machinery
Czestochowa University of Technology
Al. Armii Krajowej 21, 42-201 Czestochowa, Poland
artur.tyliszczak@pcz.pl

Bernard J. Geurts
University of Twente
P.O. Box 217
7500 AE Enschede, The Netherlands
b.j.geurts@utwente.nl

ABSTRACT

The dynamics of passively controlled turbulent flow around different bluff-bodies used in the injection system of a combustion chamber is studied using large-eddy simulation (LES). The influence of three bluff-body geometries (cylindrical, square, star) is analyzed using an in-house high-order academic code. The inlet boundary conditions are generated separately using the ANSYS Fluent software in a precursor simulation. The paper focuses on the structure of the wake, the size and shape of turbulent vortices, the size and location of the recirculation zones and the impact of these parameters on a passive scalar mixing. The performed simulations allow identification of large vortical structures formed downstream the bluff-bodies. Their topology and dynamics strongly depend on the bluff-bodies shape but the mixing intensity is not necessarily amplified when non-circular bluff-bodies are used. In the presence of sharp corners (square and star bluff-body) the small-scale vortices generated in their vicinity cause a deformation of large vortical structures and this effect leads to a less intense entrainment of the flow to the recirculation region.

INTRODUCTION

A suitable control of turbulent flow dynamics is required for establishing low-emissions and safe industrial devices (engines, burners, combustion chambers, etc.). Therefore, flow control constitutes a very important field of research both experimentally and numerically. Such control can be achieved by applying passive and/or active flow control techniques. Passive control involves manipulation of the flow field without adding any external energy. It is based on geometric shaping or adding fixed elements. Active methods involve energy input whose type and level may be fixed or vary depending on instantaneous flow behaviour. In the field of combustion, a prominent example of passive control is the use of bluff-bodies as parts of the injection systems in the combustion chambers. The bluff-body generates recirculation zones improving the mixing and stabilizing the flame position (Docquier & Candel, 2002). Their dimensions and inner structures depend on the bluff-body shape and flow parameters. Research on passive flame control often relies on a trial-and-error approach because of the largely unknown response of the flow dynamics to changes in the inlet parameters. It turns out that even small changes may drastically alter the combustion regimes. For instance, Tyliszczak *et al.* (2014) showed that a non-premixed flame stabilized in a central recirculation zone produced by a conical/circular bluff-body may extinguish following even a small change of the system parameters. Passive and active control techniques may also be combined as shown by Kypraiou *et al.* (2018). These experimental investigations focused on the impact of acoustic oscillations on bluff-body flame and their connection to a fuel injection system. Despite huge interest of the research community in the combustion instabilities, numerous questions still remain unanswered, e.g., to what extent the mixing of fuel and oxidizer downstream the bluff-body depend on the shape and roughness of the bluff-body? As it was recently found by Kuban *et al.* (2021) for jet type flows, the level of control that can be achieved in flames by nozzle shaping is higher than previously expected. Numerous works devoted to the jet configurations have been performed regarding these issues. It turns out that the jets issuing from sharp-edged orifices are more energetic compared to the jets generated by smoothly contoured nozzles, and therefore they characterise a faster axial velocity decay (Mi & Nathan, 2010; Azad *et al.*, 2012). Recent research performed by Tyliszczak *et al.* (2022) showed a different trend concerning the dynamics of the jets issuing from shaped orifices. It was presented that the shorter potential core and the faster velocity decay occur rather for a circular jet than for a non-circular one, e.g., issuing from a triangular nozzle. Similar observations were also made by Aleyasin *et al.* (2018). The discrepancies between findings reported in Tyliszczak *et al.* (2022); Aleyasin *et al.* (2018) and Mi & Nathan (2010); Azad *et al.* (2012) are attributed to differences in the constructions of nozzle ends (smooth, sharp, contraction type).

The aim of this paper is to better understand multi-scale mixing processes occurring downstream shaped bluff-body geometries. Particular attention is put on the mixing modulation, i.e., its enhancement or suppression compared to a circular shape. The mixing efficiency is crucial for flame initiation (ig-

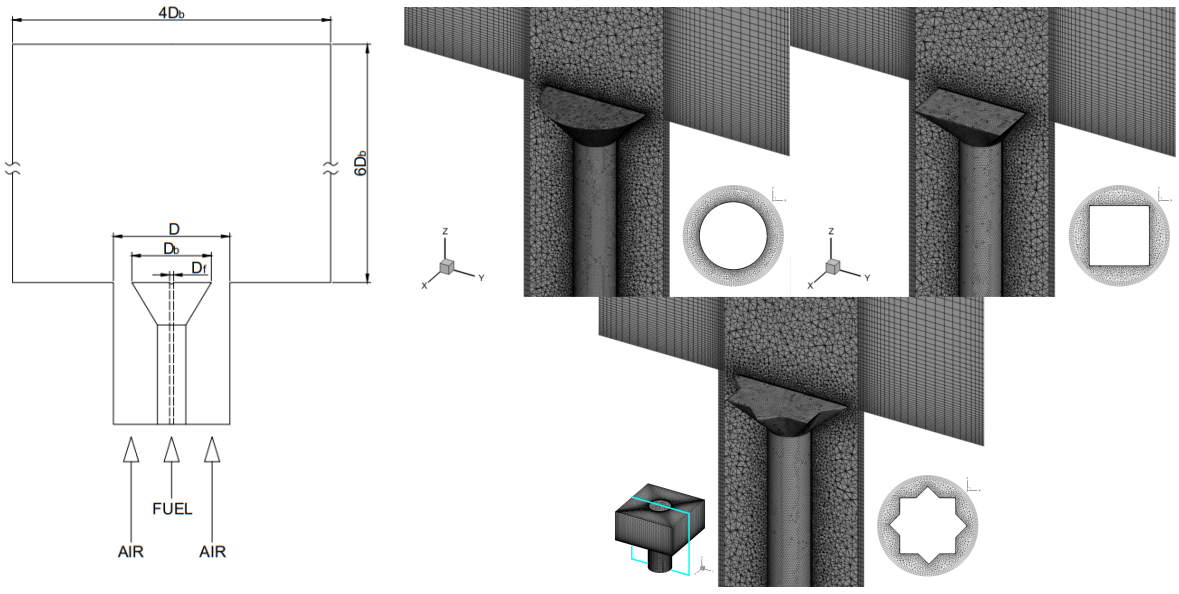

(a) (b)

Figure 1. Sketch of the bluff-body combustion chamber (a) and the bluff-body geometries (b) with the view of the computational meshes in the inlet sections for the computations performed using the ANSYS Fluent code.

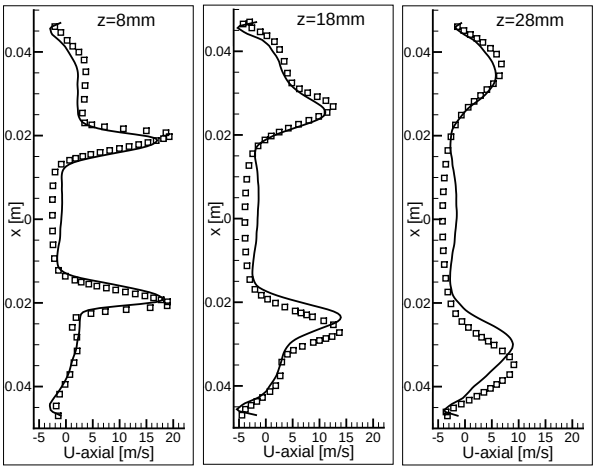

Figure 2. Axial velocity profiles downstream the circular bluff-body at various distances from the inlet plane. The symbols refer to the experimental data (Kypraiou *et al.*, 2018).

nition), propagation, or extinction. In this paper, the research is carried out using large eddy simulation (LES), which in the past has been proven to correctly capture the dynamics of this type of turbulent flow while keeping computational costs at a reasonable level. To examine and understand the response of the flow to changes of various inlet parameters associated with particular bluff-body shapes we perform the simulations for 'cold' flow conditions (no chemical reactions). The flow structure in the vicinity of bluff-bodies is analysed in detail. The ultimate aim is to answer whether it is possible to find the shape, which for a given inlet flow parameters would provide the most favourable conditions for a stable combustion process, e.g., the homogeneity of the flow and low strain rate. We examine whether using the rectangular or star shape bluff-body improves the turbulent mixing intensity with respect to the case with the circular bluff-body.

MODELLING

A schematic view of a typical combustion chamber with a conical bluff-body is shown in Fig. 1. It consists of a fuel pipe in the center and an outer section where from the bottom a co-flowing stream is provided through an inlet section with a cylindrical duct (D=37 mm). An analogous configuration has been used in experimental (Kypraiou *et al.*, 2018) and numerical (Tyliszczak *et al.*, 2014) investigations of the combustion process stability. In this paper, we modify the shape of the bluff-body assuming it as the circular, square or hexagram (star). All bluff-bodies are characterised by the same equivalent diameter D_b=25 mm (see Fig. 1), which corresponds to a circle with the surface area A the same as a given bluff-body, i.e., $D_b = 2\sqrt{A\pi}$). The research is performed for non-reacting cases focusing on changes in mixing due to changes in bluff-body shape. To mimic a situation in which both the fuel and oxidizer are provided to an injector system we introduce a mixture of hydrogen and nitrogen (5% H_2/95% N_2) that is injected into the combustion chamber through the central pipe (D_f=4

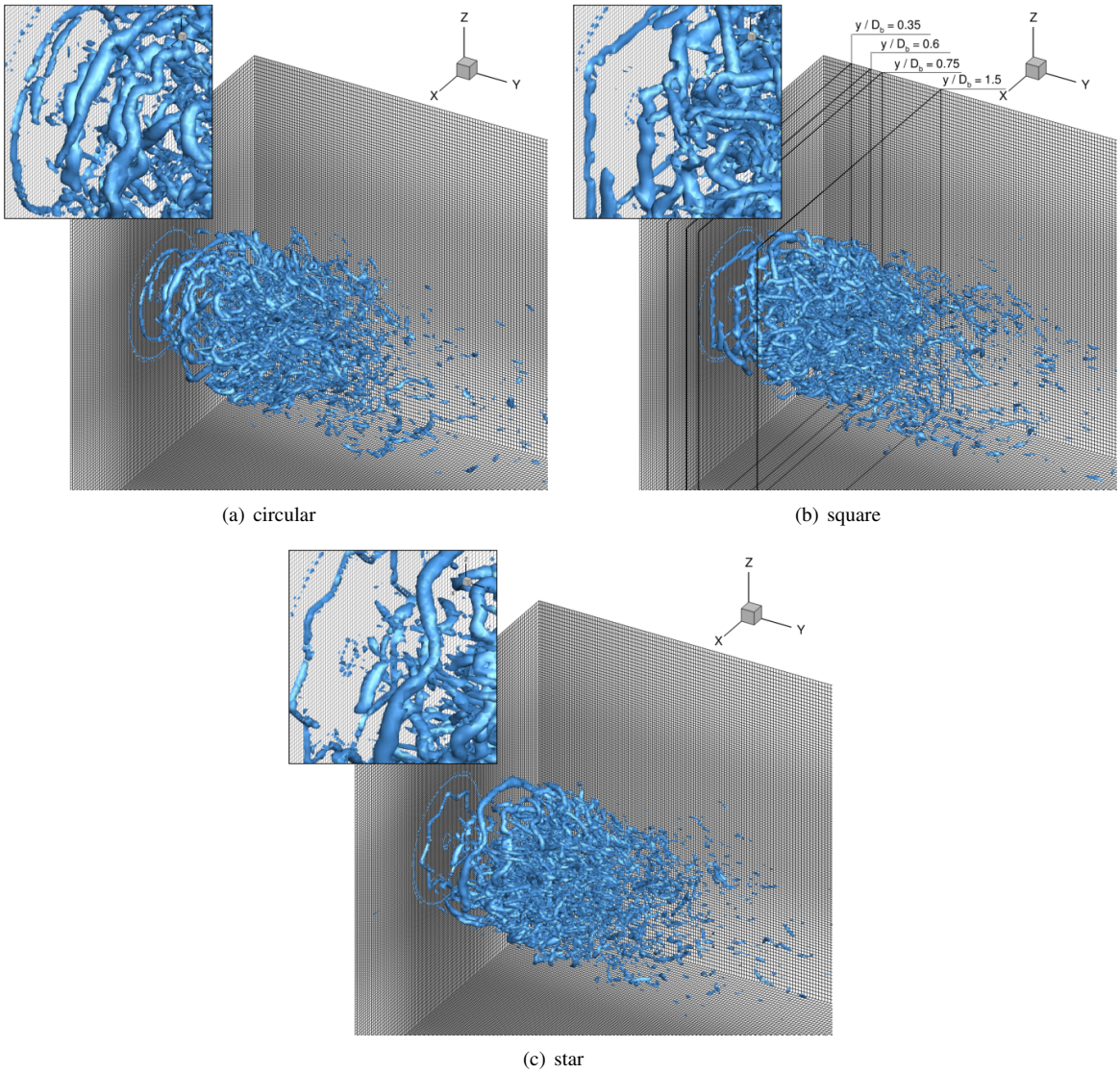

(a) circular (b) square

(c) star

Figure 3. Isosrfaces of instantaneous Q-parameter with the view of the computational meshes for the computations performed using the SAILOR code.

mm). The co-flowing oxidiser stream is air. Both, the fuel and oxidiser, have a temperature of 300 K. The stoichiometric value of the mixture fraction is $\xi_{ST} = 0.335$. Following the Bilger's definition, the mixture fraction is computed as:

$$\xi = \frac{(Y_H - Y_{H,o})/2W_H - (Y_O - Y_{O,o})W_O}{(Y_{H,f} - Y_{H,o})/2W_H - (Y_{O,f} - Y_{O,o})W_O} \quad (1)$$

where Y's are the elemental mass fractions, W's are atomic weights and the subscripts, f and o, correspond to the fuel and oxidizer stream, respectively.

The simulations are performed using a two-stage approach. In the first stage, we involve the ANSYS Fluent LES solver to model the flow inside the cylindrical inlet section, i.e., in the entrance duct and around the bluff-bodies. In these precursor calculations, we acquire unsteady velocity signals at the end of the inlet section for a period of $150D_b/U_b$ (U_b-bulk velocity of the oxidiser). In the second part, the simulations are performed using a high-order low Mach number LES solver SAILOR (Tyliszczak, 2014). The acquired velocity components are superimposed onto the inlet plane of the main computational domain involving only the outer section of the burner (see Fig. 1). It is a rectangular domain of the length $6D_b$ in the axial direction ('y') and the width $4D_b \times 4D_b$ in the 'x-z' plane. The sub-grid viscosity is computed according to a model proposed by Vreman (2004).

The numerical code SAILOR is based on the projection method for pressure-velocity coupling Tyliszczak (2014) combined with a predictor-corrector method (Adams-Bashforth / Adams-Moulton) for the time integration. The spatial discretization is performed on half-staggered meshes by the 6th order compact difference approximation for the Navier-Stokes and continuity equations. The second-order TVD (Total Variation Diminishing) scheme with Koren limiter is used for the convective terms of the species mass fraction and enthalpy transport equations. The accuracy of the SAILOR code is demonstrated in Fig. 2 showing the radial profiles of the mean axial velocity obtained for the flow configuration analysed by (Kypraiou *et al.*, 2018). In this case, an even more complicated problem than the present one was considered, it included the swirl of the incoming oxidizer stream. The velocity profiles in Fig. 2 are compared at three different axial distances from the bluff-body. A very good agreement is observed both close to the bluff-body plane (z=8 mm) as well as further downstream at z=28 mm.

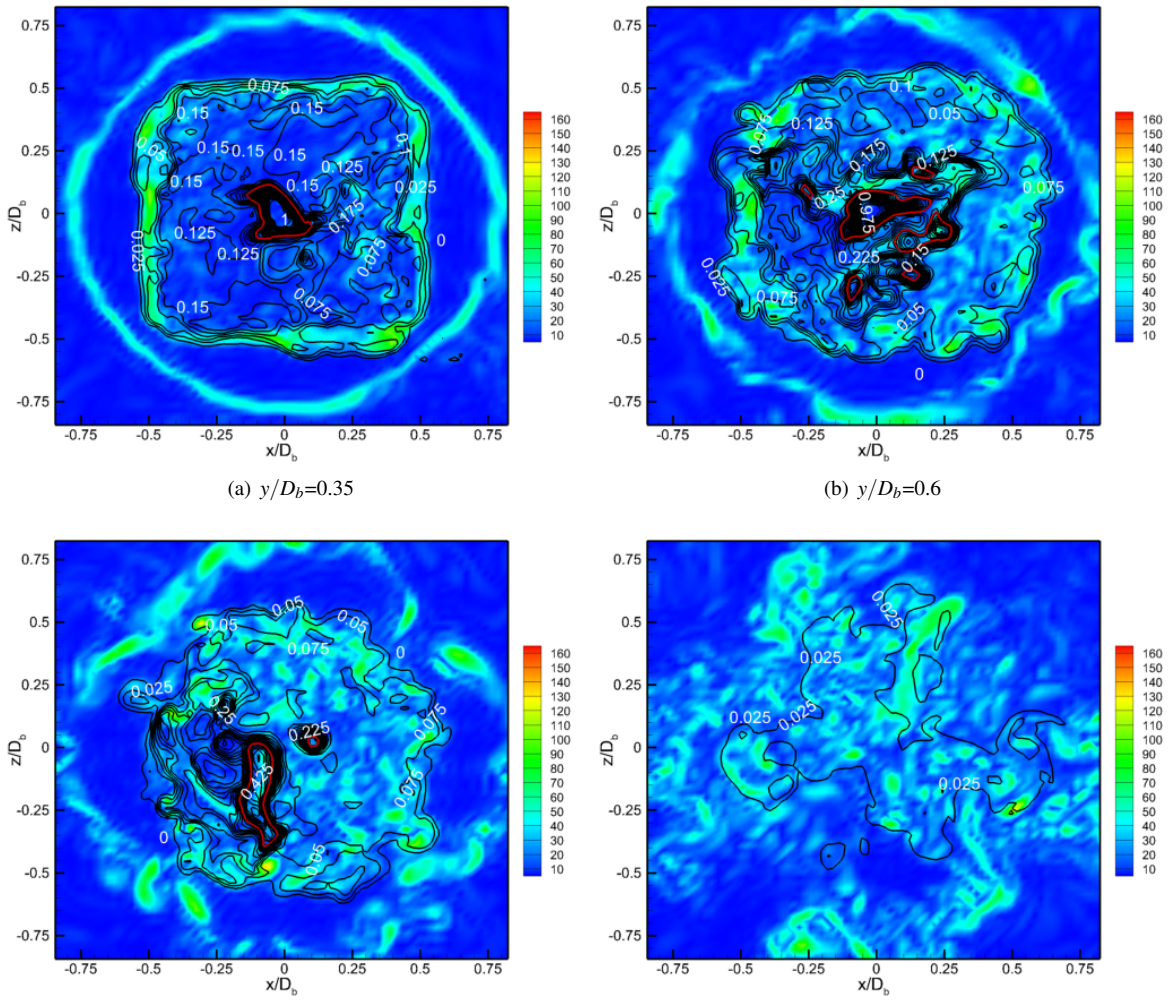

(a) y/D_b=0.35 (b) y/D_b=0.6

(c) y/D_b=0.7 (d) y/D_b=0.1.5

Figure 4. Contours of the instantaneous vorticity along with isolines of the instantaneous mixture fraction (red colour - $\xi_{ST} = 0.335$) on the 'x-z' planes depicted in Fig. 3(b).

RESULTS

The structure of the flow behind the bluff-bodies is shown in Fig. 3 presenting iso-surfaces of a constant value of the Q-parameter representing the vortical structures. Additionally, the computational mesh is presented at the sides. It is compacted towards the inlet plane and the axis. One can see in Fig. 3 that the vortices generated in the close vicinity of the inlet plane reflect the bluff-body shape. Large toroidal structures resulting from the Kelvin-Helmholtz instability, and also the accompanying smaller longitudinal vortices undergo time-space evolution. In the case of non-circular shapes, the vortices reflect the shapes of the bluff-bodies even further downstream. On the other hand, they become smaller and more irregular. The presence of small-scale vortices generated in the vicinity of sharp corners causes the deformation of large vortical structures and increases the axial velocity fluctuations that amplify the mixing process. One can expect that compared to the circular bluff-body configuration the flame structure would be different in these cases.

Figure 4 displays the vorticity contours and the mixture fraction isolines in the 'x-z' planes at different axial distances from the inlet plane of the square bluff-body. The red lines indicate the instantaneous position of the stoichiometric mixture fraction $\xi_{ST} = 0.335$. One can observe that the flow structure becomes highly irregular at the axial location $0.75D_b$. This could be already noticed by analysing the Q-parameter in Fig. 3. This is due to the non-circular sections that produce the stagnation regions and rib vortices right after the corners of the duct providing the oxidizer. As a result, the flow field is deformed significantly. The evidence of that are the contours of the instantaneous distribution of the mixture fraction. As can be seen in Fig. 4(c), they are concentrated mainly on the lower left side of the bluff-body wake.

The differences between the flows downstream of the bluff-bodies can be quantified by the comparison of the time-averaged results. Figures 5-6 show the centreline profiles of the time-averaged axial velocity and its fluctuations as well as the mixture fraction in all analysed cases. First, we focus on the profiles of the mean axial velocity component presented in Fig. 5. The results obtained using different computational grids for circular and square shapes are also included for the comparison. The labels of particular lines in the legend correspond to the number of nodes in the radial and axial directions, respectively. The use of the grid counting of 144×192 nodes provides a nearly grid-independent solution at a reasonable computational cost. It can be seen that the velocity in the near and far flow field regions is calculated with a similar accuracy on all the meshes. The results obtained using the denser mesh reveal only small differences in the axial locations where the recirculation zone ends ($y/D_b \approx 1.1$). In this paper, how-

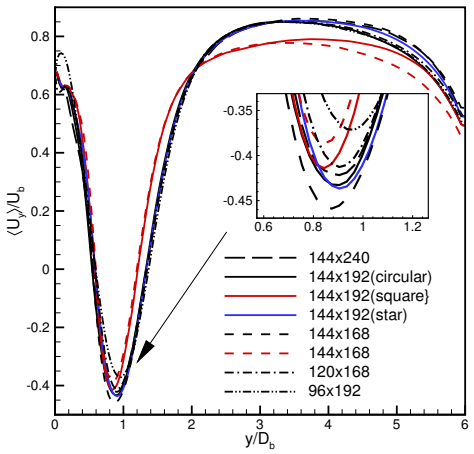

Figure 5. Profiles of the time averaged axial velocity (mean) along the axis obtained for different meshes and different bluff-bodies (black lines - circular, red lines - square, blue line - star).

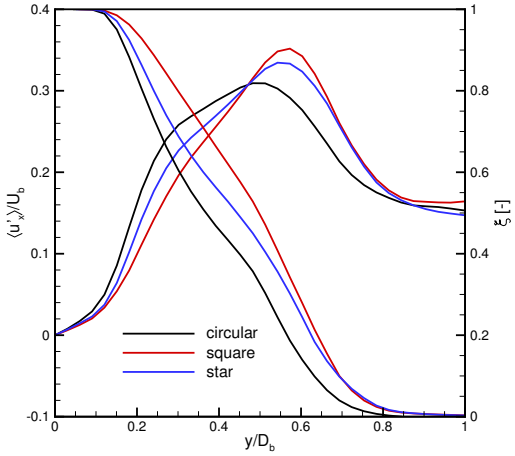

Figure 6. Profiles of the time-averaged axial velocity fluctuations and the mixture fraction along the axis.

ever, we are particularly interested in the region $y/D_b < 1.1$, as downstream of the distance $y/D_b > 1.1$ the mixture fraction level is very low, and hence, the mixing process in this part of the flow is not so important. Hence, the mesh consisting of 144×192 nodes was chosen for comparative studies.

A comparison of the velocity profiles obtained for different shapes reveals a slightly slower velocity decay in the near field region (up to $0.6D_b$) when the square bluff-body is used. Moreover, in this case the minimum velocity value is shifted towards the inlet plane by $0.1D_b$ compared to the configurations with the circular and star bluff-bodies. Worth noticing is that in the former case, the velocity drops down the fastest. Regarding the profiles of the velocity fluctuations, it can be seen that the flow behind the circular bluff-body manifests a significantly faster fluctuations increase along the axis. On the other hand, using the square bluff-body leads to the largest fluctuations maximum. The differences are at the level of $3\%U_b$, however, they become less pronounced when the flow leaves the recirculation zone.

Depending on the bluff-body shape the mixture fraction decreases slower or faster, see Figure 6. When the circular bluff-body is used the mixing is the most intense, i.e., initially large mixture fraction values drop significantly faster, compared to the two remaining cases. These results suggest that the observed flow behaviour for the bluff-bodies has some similarities with the one reported for jet flows by Tyliszczak *et al.* (2022) and Aleyasin *et al.* (2018). There, contrary to a number of investigations, the circular nozzle also turned out to be the most effective taking into account the mixing enhancement. In the present configuration, it has been found that a large amount of the oxidiser stream is taken from the surroundings and transported towards the flow axis. This effect is the most pronounced in the case of the circular bluff-body where large vortical structures seem to be the best formed. It turns out that the corners of the square and star bluff bodies make the vortical structures weaker, and thus, not so effective in transporting the oxidizer to the recirculation region. Apparently, the complex nozzle shape does not necessarily ensure a better mixing intensity.

A radial flow characteristics gives a deeper insight into the flow dynamics. The time-averaged axial velocity and mixture fraction values along the radial direction at various axial distances are presented in Fig. 7. Concerning the axial velocity, there are noticeable differences right above the bluff-bodies ($y/D_b = 0.5$) and they persist further downstream. When the square bluff-body is used the radial size of the recirculation zone is larger than in the two remaining cases. For instance, the profiles at $y/D_b = 0.5$ reveal that the recirculation zone is $0.1D_b$ wider in the location where the axial velocity is equal $U_y/U_b = 0.5$ (see the dashed line in Fig. 7(a)). In contrast to the velocity profiles the differences in the mixture fraction profiles are less pronounced and observed only in the near field (up to $y/D_b = 0.7$). One can see in Fig. 6 that the profiles diverge from each other in a near-axis region and inside the outer shear layer and overlap inside the recirculation zone where the mixing intensity is the largest. It can be concluded that the time-averaged results do not reveal such strong dependence on the bluff-body geometry as the the instantaneous solutions (see Fig. 4).

CONCLUSIONS

The paper focused on the dynamics of the flow downstream of the bluff-bodies with the aim of better understanding the scalar mixing in bluff-body stabilized burners. Three different conical bluff-body geometries were considered, i.e., the circular, rectangular and star. The research has been performed using the LES approach and two numerical codes, the ANSYS Fluent for the precursor simulations to generate the inlet boundary conditions and the high-order SAILOR code for the analysis of the scalar mixing. The performed computations revealed a smaller than expected dependence of the flow behaviour on the bluff-body shape. Instantaneous solutions showed that in the close vicinity of the bluff-body surface the large vortical structures exist and their shapes follow the ones of the bluff-bodies. This, however, did not translate on the mixing process intensity or significant changes of the velocity field in the bluff-body wake. The differences between the time-averaged solutions were less pronounced. To some extent surprising is the fact that the sharp corners of the square and star shape bluff-bodies have only a moderate impact on the flow dynamics. However, it was found that the decay of the axial velocity as well as the mixture fraction is the fastest behind the circular bluff-body. On the other hand, the use of the square bluff-body leads to the shortest but the widest recirculation zone region.

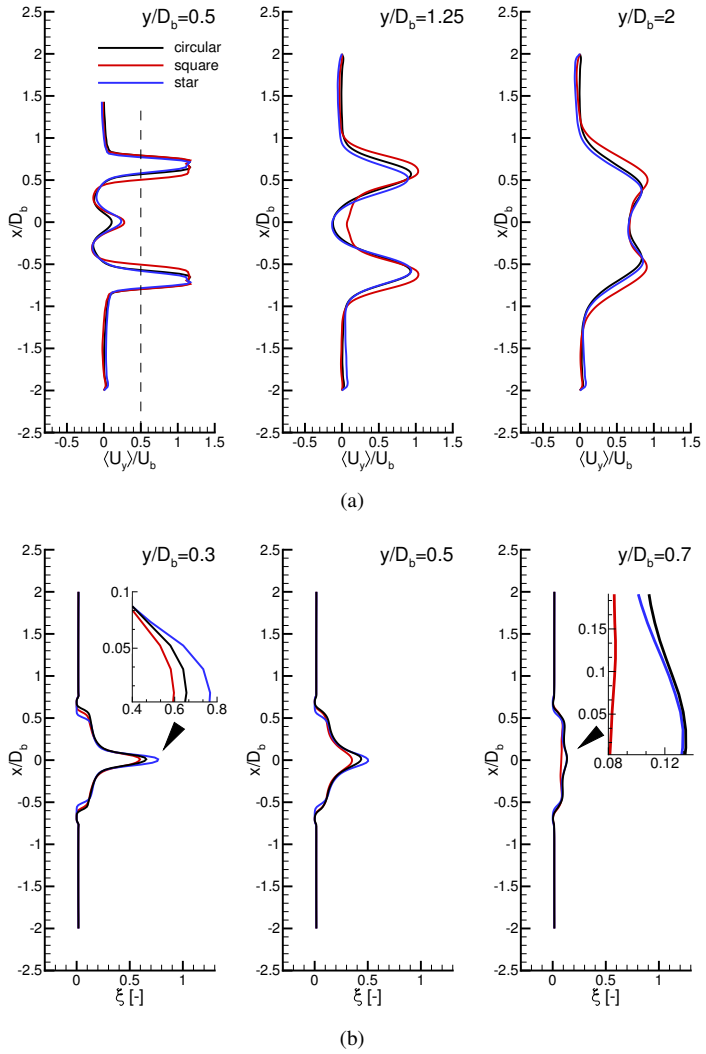

Figure 7. Radial profiles of the time averaged mean axial velocity (a) and mixture fraction (b).

ACKNOWLEDGMENTS

This work was supported by National Science Center in Poland (Grant 2020/39/B/ST8/02802) and the National Agency for Academic Exchange (NAWA) (Research project ANIMATE No. PPI/APM/2019/1/00062). The computations were carried out using PL-Grid Infrastructure.

REFERENCES

Aleyasin, S.S., Fathi, N., Tachie, M.F., Vorobieff, P. & Koupriyanov, M. 2018 On the development of incompressible round and equilateral triangular jets due to reynolds number variation. *Journal of Fluids Engineering* **140** (11).

Azad, M., Quinn, W.R. & Groulx, D. 2012 Mixing in turbulent free jets issuing from isosceles triangular orifices with different apex angles. *Experimental Thermal and Fluid Science* **39**, 237–251.

Docquier, N. & Candel, S. 2002 Combustion control and sensors: a review. *Progress in Energy and Combustion Science* **28** (2), 107–150.

Kuban, L., Stempka, J. & Tyliszczak, A. 2021 Numerical analysis of the combustion dynamics of passively controlled jets issuing from polygonal nozzles. *Energies* **14** (3), 554.

Kypraiou, A.M., Allison, P.M., Giusti, A. & Mastorakos, E. 2018 Response of flames with different degrees of premixedness to acoustic oscillations. *Combustion Science and Technology* **190** (8), 1426–1441.

Mi, J. & Nathan, G.J. 2010 Statistical properties of turbulent free jets issuing from nine differently-shaped nozzles. *Flow, Turbulence and Combustion* **84** (4), 583–606.

Tyliszczak, A. 2014 A high-order compact difference algorithm for half-staggered grids for laminar and turbulent incompressible flows. *Journal of Computational Physics* **276**, 438–467.

Tyliszczak, A., Cavaliere, D.E. & Mastorakos, E. 2014 LES/CMC of blow-off in a liquid fueled swirl burner. *Flow, Turbulence and Combustion* **92** (1-2), 237–267.

Tyliszczak, A., Kuban, L. & Stempka, J. 2022 Numerical analysis of non-excited and excited jets issuing from non-circular nozzles. *International Journal of Heat and Fluid Flow* **94**, 108944.

Vreman, A.W. 2004 An eddy-viscosity subgrid-scale model for turbulent shear flow: Algebraic theory and applications. *Physics of Fluids (1994-present)* **16** (10), 3670–3681.